Detection of Sclerotic Bone Metastases in the Spine Using Watershed Algorithm and Graph Cut

Tatjana Wiese[1], Jianhua Yao[1], Joseph E. Burns[2] and Ronald M. Summers[1]

1. Radiology and Imaging Sciences Department, Clinical Center, National Institutes of Health, Bethesda, MD 20892
jyao@cc.nih.gov
2. Department of Radiological Sciences, University of California, Irvine, CA 92868

ABSTRACT

The early detection of bone metastases is important for determining the prognosis and treatment of a patient. We developed a CAD system which detects sclerotic bone metastases in the spine on CT images. After the spine is segmented from the image, a watershed algorithm detects lesion candidates. The over-segmentation problem of the watershed algorithm is addressed by the novel incorporation of a graph-cuts driven merger. 30 quantitative features for each detection are computed to train a support vector machine (SVM) classifier. The classifier was trained on 12 clinical cases and tested on 10 independent clinical cases. Ground truth lesions were manually segmented by an expert. The system prior to classification detected 87% (72/83) of the manually segmented lesions with volume greater than 300 mm^3. On the independent test set, the sensitivity was 71.2% (95% confidence interval (63.1%, 77.3%)) with 8.8 false positives per case.

Keywords: sclerotic bone metastasis, watershed algorithm, graph cut, computer-aided detection

1. INTRODUCTION

Bone metastases are significantly associated with cancer, with occurrence in up to 70% of people afflicted with advanced prostate and breast cancer. Approximately 350,000 people in the United States die with bone metastases each year [1]. The tumor burden at the time of death in patients with advanced breast or prostate cancer is likely to be mostly in bone for reasons including the high blood flow in red marrow regions, the angiogenic and bone-resorbing factors produced by tumor cells when they bind to stromal cells in the marrow and to the bone matrix, and immobilized growth factors in the bone that help the tumor cells grow [1]. The morbidity is often debilitating: bone metastases can result in severe bone pain, pathological fractures often in load-bearing bones, and spinal cord and other nerve compression [1]. Moreover, no more than 20% of breast cancer patients survive more than five years after the initial discovery of the metastasis [1]. Thus the early detection of bone metastases has significant clinical importance. For example in the case of prostate cancer, the prognosis and treatment regime for the patient changes from curative to palliative when prostate tumor cells are discovered in the skeleton [1]. The spine is an essential support structure for the upper body and plays an indispensable part in protecting the spinal cord. Therefore we begin our study of bone metastases with the spine.

Medical Imaging 2012: Computer-Aided Diagnosis, edited by Bram van Ginneken, Carol L. Novak,
Proc. of SPIE Vol. 8315, 831512 · © 2012 SPIE · CCC code: 1605-7422/12/$18 · doi: 10.1117/12.911700

The broadest classification of bone metastases based on the radiographic and tomographic appearance consists of osteolytic (also known as lytic) and osteoblastic (also known as sclerotic) metastases [2]. Osteolytic metastases are characterized by decreased bone density due to the destruction of bone tissue, whereas sclerotic metastases consist of hyperdense bone regions [1]. Generally, a cancer patient with osseous metastatic disease may present with either type of lesion, and the metastases can be predominantly lytic or predominantly sclerotic depending on the type of cancer. For example, metastases caused by breast cancer are usually lytic, whereas metastases caused by prostate cancer are usually sclerotic [1]. Sclerotic lesions are believed to be caused by the production of growth factors that encourage osteoblast proliferation, differentiation, and bone formation [1]. A similar study to this one, which presents a CAD system for detecting lytic bone lesions in the spine, has been previously conducted [2]. Our purpose is to expand upon this study by developing CAD software for the detection of sclerotic osseous metastases in the spine, as an initial foray into a broader study of computational analysis of neoplastic and traumatic bone lesions. This investigation is focusing on sclerotic metastases in spine. Examples of sclerotic metastases are shown in Figure 1.

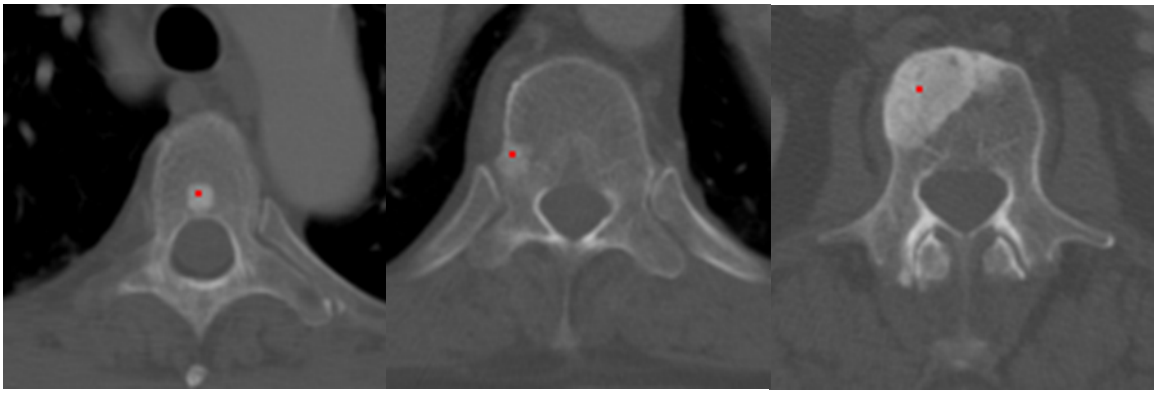

Figure 1. Examples of sclerotic metastases in spine from three different patients
Red dots indicate the center of a lesion. The first two are on thoracic spine, and third one is on lumbar spine.

The paper is organized as follows. Section 2 describes the method. Section 3 presents the data and results. Section 4 concludes the paper with some discussions.

2 METHODS

2.1 Method overview

The flow chart of our system is shown in Figure 2. Our approach consists of three stages: 1) preprocessing; 2) lesion detection; and 3) classification. The processing stage segments and partitions the spine and limits the search region for further detection. The detection stage detects and segments potential lesions. At the end, quantitative features are computed for detections and sent to a classifier to determine whether they are true or false lesions. The classifier is generated using manually labeled data as ground truth.

2.2 Preprocessing

In the preprocessing stage, the spine is segmented via thresholding and region growing. The spinal canal is extracted using a directed graph search. The vertebral borders are further refined

using a vertebra template. Based on the segmentation result, the spine is then divided into different regions: vertebral body, transverse process, spinous process, spinal canal and intervertebral disk. The detail of the spine segmentation algorithm can be found in [3]. Figure 3 shows the results of spine segmentation.

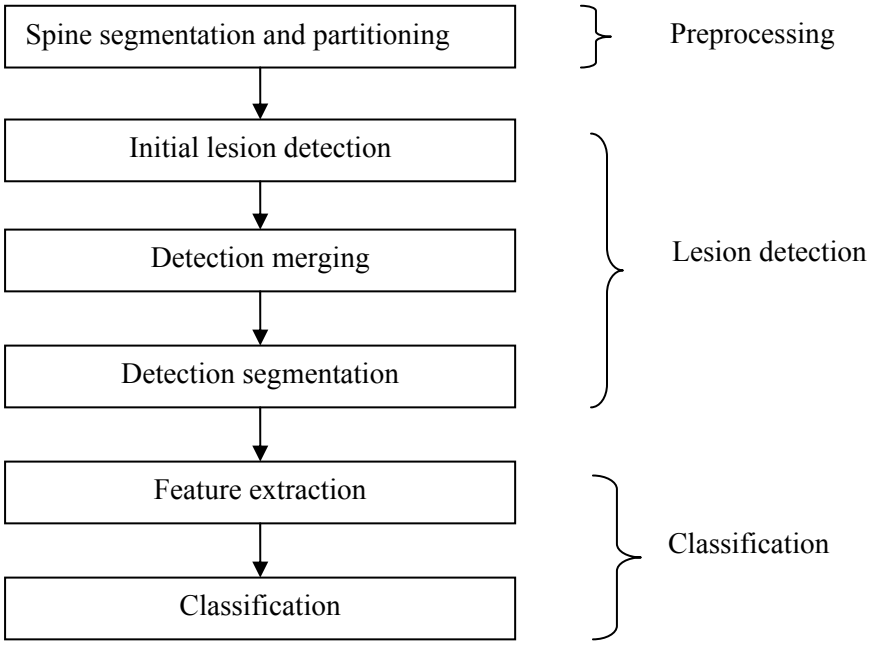

Figure 2. Flow chart

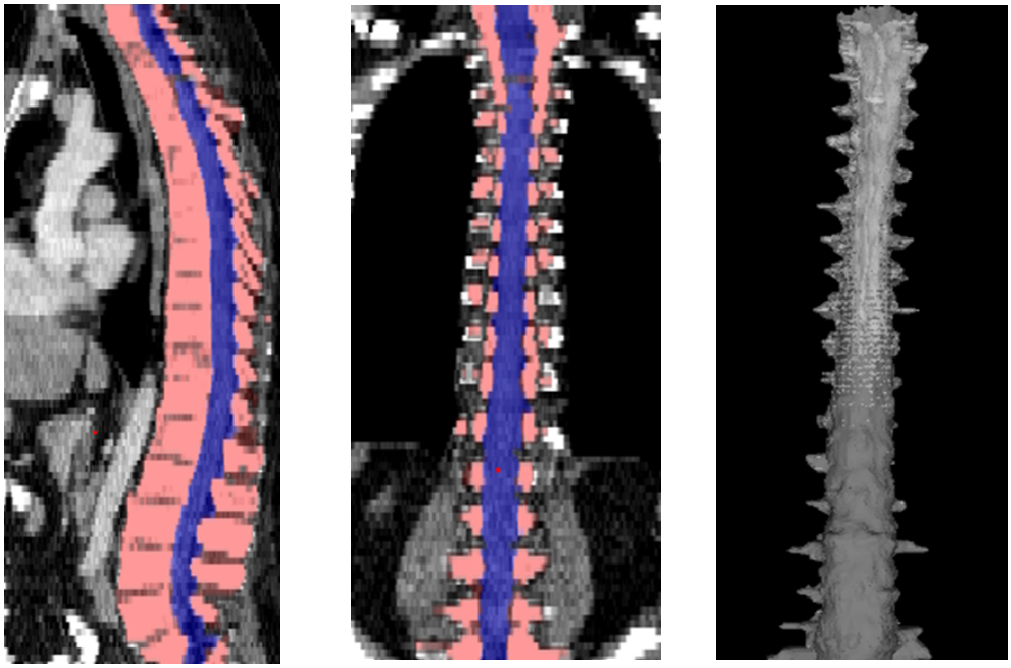

Figure 3. Spine segmentation
Red: spine region, blue: spinal canal.

2.3 Lesion Detection

After the pre-processing stage, we locate potential sclerotic bone metastases in three steps. First a watershed algorithm is applied to extract candidates, followed by a merging routine based on graph cut to avoid oversegmentation. The resulting 2-D candidates are then merged into 3-D candidate detections. For each 3-D candidate, a set of features is computed, and resulting size measurements are passed through a detection filter. The candidates which successfully pass through the detection filter are then sent to the next stage.

The watershed algorithm [4] views the gradient of the image intensity as a topographic surface in order to extract relatively homogeneous regions of the image called catchment basins, some of which will be candidates for sclerotic lesions. Example results of the watershed algorithm are shown in Figure 4.

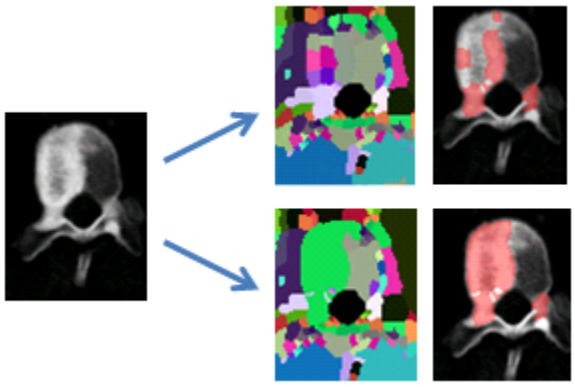

Figure 4. Watershed and graph cut algorithm. Left: Sclerotic lesion. Top arrow: The watershed regions are too differentiated, so the entire lesion is not found. Left: watershed segmentation with no merging; Right: detections with no merging. Bottom arrow: The entire lesion is found after graph cut merging. Left: watershed segmentation after merging; Right: detections after merging. There are two lesions in the vertebra, both are detected.

We then address the over-segmentation problem in watershed with a post-watershed merging routine using a graph-cuts strategy [5]. We first initialize each watershed region with a foreground (F) or background (B) label. There are two types of foreground regions: those in the cortical bone region and those in the medullary regions. Any region that has intensity 100 HU higher than its surrounding regions (cortical or medullary) will be initialized as F. The rest of the regions are initialized as B. The regions and their neighbors are fed into a graph-cuts merging routine.

An adjacency graph for watershed regions is constructed by representing adjacent regions as nodes connected by edges [6]. The technique partitions the set of nodes into two disjoint sets F and B in a manner that minimizes an energy function,

$$E(L) = \sum_{\{p,q\}\in N} V_{Lp,Lq}(p,q) + \sum_{p\in P} D_{Lp}(p) \qquad (1)$$

where P is the set of watershed regions, N is the set of pairs of adjacent regions, L is a labeling of all the regions where a given region p can have the label $L_p=F$ or $L_p=B$, V is a smoothness term that penalizes regions with similar densities having different labels, and D is a data term that penalizes a region with low density marked as foreground, or a region with high density marked

as background. Thus the technique will merge higher-density regions into the foreground, and lower-density regions into the background. In this case,

$$D_B(p) = K_B sign(I(p) - m_B)(I(p) - m_B)^2$$
$$D_F(p) = K_F sign(m_F - I(p))(I(p) - m_F)^2 \quad , \qquad (2)$$

where K_F=100, K_B=1 in our setting, $I(p)$ is the mean intensity of region p, and m_B and m_F are the means of the background and foreground respectively. As for the smoothness term, we chose

$$V_{Lp,Lq}(p,q) = K_s e^{-H^2/2\delta_s^2} \qquad (3)$$

where $K_s = (\delta_F + \delta_B)/2$, δ_F and δ_B are the standard deviation of the foreground and background respectively. $H = \sum_r | H_p^r - H_q^r |$ and $H_p^r = \sum_{t \le r} h_p^t$ are the cumulative histogram of region p, and $\delta_s = 10000$.

The smoothness and data penalty functions provide edge weights *w(i,j)* for a graph *G* consisting of the adjacency graph of the watershed regions and two additional nodes *f* and *b* which both have edges connecting them to every region node:

$$w(f, q) = D_F(q); \quad w(p, b) = D_B(p); \quad w(p,q) = V_{Lp,Lq}(p, q) \qquad (4)$$

A graph cut $\{F, B\}$ is a partition of the set of nodes such that $f \in F$ and $b \in B$, and the value of the cut is

$$c(F, B) = \sum_{i \in F, j \in B} w(i, j) \quad . \qquad (5)$$

A minimal graph cut of *G* is equivalent to a labeling that minimizes Eq. (1). Such a cut is computed according to a max-flow algorithm referenced in which generates a local minimum within a known factor of the global minimum. The resulting partition $\{F, B\}$ yields an optimized way of merging watershed regions in which regions corresponding to nodes in *F* and *B* are labeled as *F* and *B* respectively. Fig. 1 demonstrates the effect of this merger. Each merged *F* region is then regarded as one potential detection.

2.4 Feature Extraction and Classification

Next, a set of 30 quantitative features based on shape, intensity, and location is computed. Example features include volume, mean intensity, and sphericity. Table 1 lists all the features. The features are sent to a support vector machine (SVM) classifier for classification [7].

Table 1. Quantitative features

Shape	Density	Location
surfaceArea	meanIntensity	distToBoundary
volume	stdevIntensity	relCoordx
primaryAxisLength	skewnessIntensity	relCoordy
secondaryAxisLength	kurtosisIntensity	onPedicle
aspectRatio10	interiorIntensity	bbPart
aspectRatio20	borderIntensity	outerBorderRatio
aspectRatio21	outsideIntensity	bboxBorderRatio
spherecity	outsideIntensityDev	corticalBorderRatio
shapeComplexity_f1	innerOuterContrast	cordBorderRatio
shapeComplexity_f2	neighborIntensity	
shapeComplexity_f21		

3 RESULTS

A series of CT scans from 22 patients with studies demonstrating sclerotic metastatic disease in the spine was gathered. There were 18 patients (82%) with prostate cancer, two patients (9%) with lung cancer, and two patients (9%) with breast cancer. The cases were obtained from an electronic medical record search of the NIH Clinical Center in the period July 2009-2010. The patient age ranged from 50-75 years, with an average of 64.6 years. The slice thickness was 5mm. 12 cases were used for training and 10 for testing. All but two of the test cases, used for controls, demonstrated at least one sclerotic lesion in the spine.

The lesions were identified, marked and manually segmented by an expert radiologist. The training set has 216 lesions, 180 of them greater than 300 mm^3. The test set has 117 lesions, 83 of them greater than 300 mm^3.

The pre-classifier program detected 72/83 ground truth lesions with volume greater than 300 mm^3 in the test set. The overall system performance is 71.2% sensitivity with a 95% confidence interval of (0.631, 0.773), at an average of 8.8 false positives per patient. The area under the curve (AUC) is 0.814, with a 95% confidence interval of (0.787, 0.833). Figure 5 shows the results and typical examples of false positives. Figure 6 shows the FROC curve.

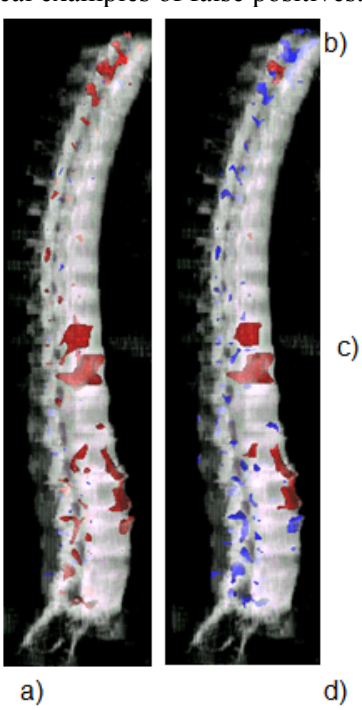

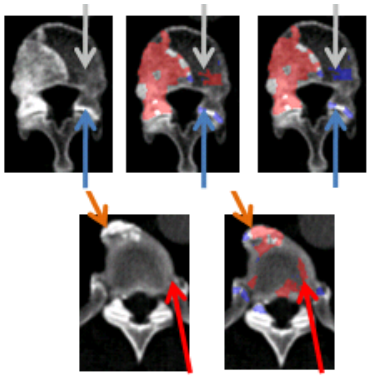

d)

	> 0 mm^3	>300 mm^3	> 0 mm^3	>300 mm^3
GT	117	83	216	180
Pre-SVM	68.4%	86.8%	80.1%	87.2%
Post-SVM	55.8% (FP: 7.53)	71.2% (FP: 8.76)	69.3% (FP: 9.03)	76.7% (FP: 9.59)

Figure 5. Performance of our CAD system. a) 3D rendering of detection results. Left: pre-SVM, right: post-SVM. Red: true positives, blue: false positives as determined by SVM. b) Detections at three stages of the program: initial, pre-SVM, post-SVM. Gray arrows: false positive discarded by SVM, blue arrows: false positive excluded by feature filters. c) Two types of false positives. Orange arrows: degenerative change, red arrows: endplate. d) Quantitative results for training (right) and testing data (left). The results are shown as sensitivity (false positive rate). GT = ground truth.

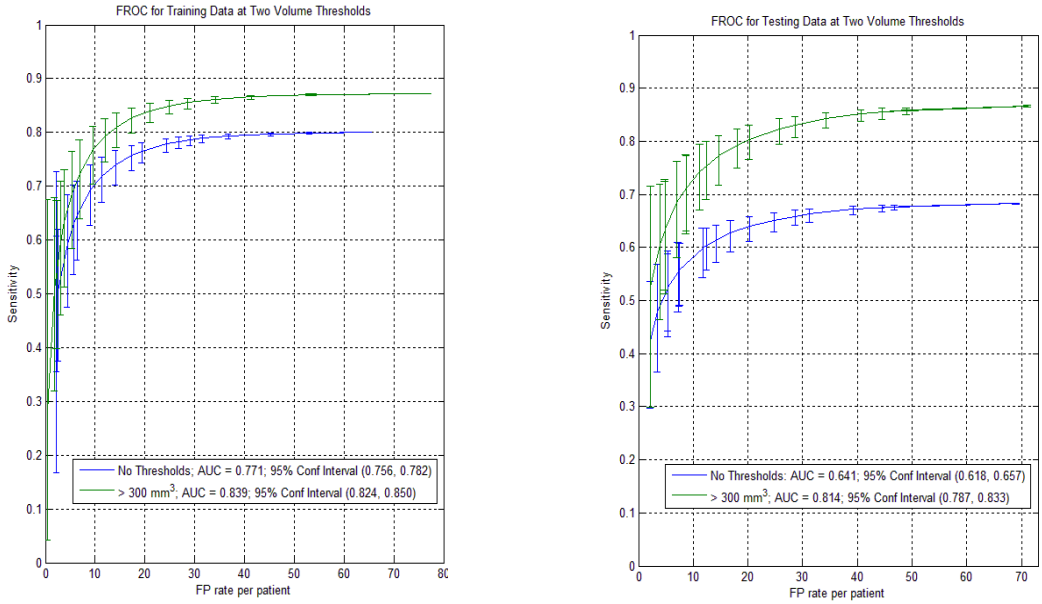

Figure 6. FROC curves of SVM performance. Left: Training data, right: testing data.

4 CONCLUSIONS

We developed a CAD system which detects sclerotic bone metastases in the spine on CT images. The CAD system shows promising results. Our CAD system includes the incorporation of a novel graph cuts region merging algorithm and a three-dimensional lesion feature computation function. The graph cuts algorithm takes into account the global information of each vertebral body to optimize image segment labeling.

ACKNOWLEDGEMENTS

This work was supported by the Intramural Research Program at National Institutes of Health, Clinical Center.

REFERENCES

[1] G. Mundy, "Metastasis to bone: causes, consequences and therapeutic opportunities," *Nature Reviews Cancer*, vol. 2, pp. 584-593, 2002.

[2] C. Whyne, M. Hardisty, F. Wu, and T. Skrinskas, "Quantitative characterization of metastatic disease in the spine. Part II. Histogram-based analyses," *Med Phys*, vol. 34, pp. 3279-3285, 2007.

[3] S. D. O'Connor, J. Yao, and R. M. Summers, "Lytic Metastases in Thoracolumbar Spine: Computer Aided Detection at CT -- A Preliminary Study," *Radiology*, vol. 242, pp. 811-816, 2007.

[4] L. Vincent and P. Soille, "Watersheds in Digital Spaces: An Efficient Algorithm Based on Immersion Simulations," *IEEE Trans. Pattern Anal. Machine Intell.*, vol. 13, pp. 583-598, 1991.

[5] J. Stawiaski and E. Decencière, "Region Merging Via Graph-Cuts," *Image Anal Stereol* vol. 27, pp. 39-45, 2008.

[6] Y. Boykov and V. Kolmogorov, "An Experimental Comparison of Min-Cut/Max-Flow Algorithms for Energy Minimization in Vision," *IEEE Pattern Analysis and Machine Intelligence*, vol. 26, pp. 1124-1137, 2004.

[7] J. Yao, R. M. Summers, and A. K. Hara, "Optimizing the Support Vector Machines (SVM) Committee Configuration in Colonic Polyp CAD System," presented at SPIE Medical Imaging, San Diego, CA, 2005.